

A K-Means Segmentation Method for Finding 2-D Object Areas Based on 3-D Image Stacks Obtained by Confocal Microscopy

Antti Niemistö^{*†‡}, Tomi Korpelainen^{†‡}, Ramsey Saleem^{*},
Olli Yli-Harja[†], John Aitchison^{*}, and Ilya Shmulevich^{*}

^{*}Institute for Systems Biology, Seattle, Washington, USA

[†]Institute of Signal Processing, Tampere University of Technology, Tampere, Finland

[‡]Equal contributors

Abstract—A segmentation method for three-dimensional image stacks obtained by confocal microscopy is proposed. The method can be used to find two-dimensional object areas based on an image stack. The segmentation method is based on K-means clustering, global thresholding, and mathematical morphology. As a case study, the proposed method is applied to 244 image stacks of the yeast *Saccharomyces cerevisiae*. Quantitative comparisons with manually obtained results as well as with results obtained by a two-dimensional segmentation method are used to illustrate how the additional information provided by three-dimensional image stacks can improve segmentation results.

Index Terms—Image analysis, segmentation, K-means clustering, thresholding, mathematical morphology, three-dimensional, image stack, confocal microscope, yeast

I. INTRODUCTION

Because real world objects are three-dimensional, confocal microscopy is increasingly being used to obtain three-dimensional image data in the form of an image stack. An image stack consists of a number of two-dimensional images, each imaged at a specific focal plane. These images are often referred to as z -slices of the stack. This paper presents a K-means segmentation method for finding the object locations based on such three-dimensional image data. The goal is to find a two-dimensional binary mask that defines the object locations. In principle, segmentation is possible based on a single z -slice only, but, as shown here, the use of additional z -slices gives new information on cell locations, and thus helps to improve the accuracy of segmentation.

In this paper we use images of the budding yeast *Saccharomyces cerevisiae* as a case study to illustrate our K-means segmentation method. Although a two-dimensional mask cannot be used to describe the three-dimensional size or shape of the cells in the image, it can be used as a location marker for detecting subcellular structures. The two-dimensional mask can be thought of as defining a cylinder in the three-dimensional space, and subcellular structures are found from the space defined by this cylinder. This is typically done by multimodal microscopy, meaning that cells are imaged in one channel (often transmission imaging) and organelles are imaged in another channel (often fluorescent).

The yeast *S. cerevisiae* is an important model organism, and imaging is increasingly applied in studies on yeast, including morphology, cell cycle, signaling pathway, and gene function studies [1]–[7]. In many studies extensive

manual analysis is performed on the images, and in others semi-automated image analysis methods are used. However, fully automated methods should be favored over manual and semi-automated methods, since without full automation human factors such as fatigue and distraction result in errors in the analysis results, leading to inter-user as well as intra-user variability in the results. Moreover, modern high-throughput experiment and imaging technologies produce vast amounts of image data, calling for fully automated methods for producing reliable image analysis results in a reasonable time.

The first step of most image analysis tasks is the segmentation of the objects of interest from the background. Considerable efforts have been made to enable fully automated segmentation of yeast cells; see, for example, [2], [3], [8]–[12]. These papers have also considered the problem of detecting clustered cells individually by applying region splitting methods. All these papers have considered the segmentation problem in two dimensions.

The K-means segmentation method is presented in Section II. The results obtained with this method are analyzed in detail in Section III, using a set of 244 confocal image stacks. The results are also compared with results obtained by manual analysis done by visual inspection of the images as well as with results obtained by a simple modification of the image analysis method that we have previously presented for two-dimensional images [10]. The implications of the obtained results are discussed in Section IV.

II. METHODS

A. Experimental procedure and image acquisition

A total of 34 strains of the yeast *S. cerevisiae* were grown in YEPD (1% yeast extract, 2% peptone, and 2% glucose) overnight, then transferred to SCIM medium (0.7% yeast nitrogen base, 0.5% yeast extract, 0.5% peptone, 0.5% Tween 40, 0.79 g/L of complete synthetic medium (Qbiogene, Morgan Irvine, CA, USA), 0.5% $(\text{NH}_4)_2\text{SO}_4$, 0.1% glucose, and 0.15% oleic acid) and induced for 4 hours. Post induction, cells were fixed with 3.7% formaldehyde for 30 minutes, then washed three times with phosphate buffered saline solution. The cells were visualized using a Leica confocal microscope using transmission imaging with a 100x oil immersion objective (NA 1.40). In total 244 stacks of 20 z -slices of size 512×512 pixels (8 bits per pixel) were

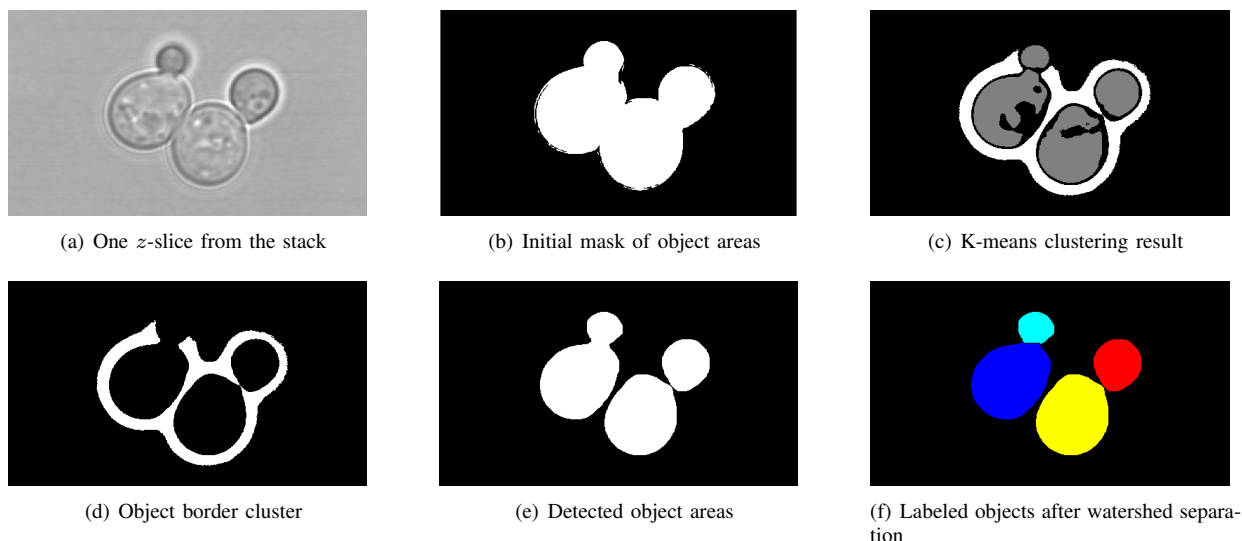


Fig. 1. A 512×292 part of an image stack at different image processing stages.

obtained. As an example, the tenth z -slice from one of the obtained stacks is shown in Fig. 1(a).

B. *K-means segmentation in three dimensions*

Our K-means segmentation method has three main steps. First, an initial mask of the object areas is obtained. The mask is merely a cover of all the objects in the image stack: at this point separation of touching objects is not attempted. The second step is the segmentation of the object borders, which is done by K-means clustering [13]. In the third step these binary images are combined by the logical AND operation between the mask image and the negative of the border image. This three-step method, followed by a number of post-processing steps (see Section II-C), allows us to obtain a good segmentation result even if there are discontinuities in the object borders segmented in the second step.

The initial mask of the object areas is obtained as follows. First, the local variance image of each z -slice is obtained, and the resulting 20 images are summed together. Then, the resulting image is thresholded using the threshold value $t = 0.5t_o$, where t_o is obtained by Otsu's method [14]. The mask obtained for our example image stack is shown in Fig. 1(b).

In the second step we consider the different z -slices of the stack to be features of the information given by the stack. Since we have 20 z -slices, we have a feature vector of 20 features for each xy -location. K-means clustering with three clusters is applied, and the result for our example image stack is shown in Fig. 1(c). We use the cosine distance measure in K-means clustering. The cosine distance measure depends on the direction of the feature vectors and is independent of their magnitude. This is a desirable property, since the directions of the feature vectors representing the background, cell membranes, and intracellular parts fall into three distinct clusters. Random initialization of the cluster centroids can be used, but it sometimes causes the K-means clustering method to converge at a local minimum rather than the global minimum. To avoid this, the cluster centroids should

be initialized by first clustering just one image stack with random initial centroid locations. If the clustering result is satisfactory according to visual inspection, the obtained cluster centroids can be used as an initialization for similar image stacks. This procedure can be thought of as a simple teaching phase, and typically just a single iteration in the teaching phase is needed to obtain significant improvement in the clustering results.

The decision on which of the clusters is the object border cluster can be made as follows. First, the background cluster is excluded. In our case study with yeast images this is equivalent to excluding the largest cluster. After this we make the logical AND operation between the mask and a cluster, and calculate the ratio between the resulting area and the area of the cluster. These operations are done to the two clusters that remain after the background cluster is excluded, and the object border cluster is the one for which the ratio is smaller. The object border cluster is shown in Fig. 1(d).

The result of subtracting the binary image of the object borders obtained in step two (Fig. 1(d)) from the initial mask obtained in step one (Fig. 1(b)) is shown in Fig. 1(e). Note that since some of the object borders detected in step two have discontinuities, some touching objects have not been separated at this point.

C. *Post-processing*

The cluster consisting mainly of the object borders may include some other regions inside the objects. These unwanted regions result in holes in the objects of the binary image obtained in step three of the K-means segmentation method. Therefore, we employ the morphological reconstruction to perform a simple flood fill of these holes. As a second post-processing step, touching objects that are falsely recognized as a single object are separated by the classic watershed separation method. The result for our example image stack is shown in Fig. 1(f). In addition, predefined minimum and maximum object size thresholds are enforced to remove

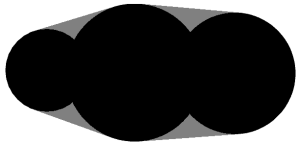


Fig. 2. A concave object (black) and the concave area (gray) of its convex hull (black and gray).

objects that are likely to be false positives. The image border is also cleared of objects. Apart from watershed separation, these final steps do not have any effect on the segmentation result of our example image stack, but are needed for some of the other stacks that are part of our case study.

D. Segmentation in two dimensions

We have previously published a segmentation method for two-dimensional yeast images [10]. This method can be directly applied to the each of the 20 z -slices of the image stacks used in this paper. The results for the z -slices that are close to the one where the cells are in the best focus are very similar to the results obtained by the K-means segmentation method proposed in this paper. Therefore, we implemented a simple scheme that uses certain heuristics, described below, to select the best segmentation result from the 20 that are obtained when each z -slice is segmented separately. We then compared the obtained results with the results obtained with the K-means segmentation method.

Since we know that yeast cells are generally convex objects, convexity is the main heuristic that we use to select the best segmentation result. We calculate for each segmented z -slice the number of pixels in the concave areas of the objects (see Fig. 2). The z -slices for which this number is low are candidates for the best segmentation result. In addition, we also look at the number of cells found in each z -slice. A z -slice that has a small number of concave area pixels and a high cell count is selected as our best segmentation result. With the image stacks used in our case study, we decided to consider as candidates those z -slices that have at most $1.5N_c$ concave area pixels, where N_c is the number of concave area pixels in the z -slice that has the smallest number of concave area pixels. From these z -slices we select the one that has the largest number of detected cells. If several z -slices have the same cell count, we select the one that has the smallest number of concave area pixels.

The labeled segmentation result obtained by the above method for the example image stack used in Fig. 1 is shown in Fig. 3. The post-processing steps used to obtain this image are the same as those used to obtain the image in Fig. 1(f) (see Section II-C).

III. RESULTS

According to manual analysis, the 244 image stacks that are used in this paper contain a total of 1668 cells with the mean count 6.8 (standard deviation 2.86, and median as well as mode 6). The minimum number of cells in a single stack is 1 and the maximum is 18. Fig. 4 shows the

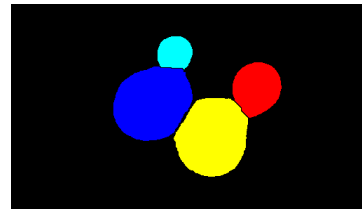


Fig. 3. Labeled segmentation result for the example image stack using the two-dimensional segmentation method.

scatter plot of automated cell counts obtained with the K-means segmentation method vs. the manual cell counts. Each dot represents one or more images, and the number on the right of each dot refers to the number of image stacks that produced a particular manual and automated count pair. The number of images is also color-coded on the dots.

The scatter plot indicates that the cell counts obtained with the K-means method match the manual cell counts for 199 (81.6%) image stacks. For 8 (3.3%) image stacks the K-means method gives a count that is higher by one cell. The counts are lower by 1, 2, and 3 cells for 26 (10.6%), 9 (3.7%), and 2 (0.8%) image stacks, respectively. The mean absolute error is 0.24. These data as well as visual inspection of the segmentation results (data not shown) suggests that the K-means segmentation method gives very accurate results. Most of the segmentation errors result from cells that are not in good focus in any of the z -slices. It should also be noted that in these cases counting the cells manually is difficult, and these manual counts may be incorrect. By visual analysis of the segmentation results we were also able to confirm that there are very few cases in which there are false negatives and false positives (which would cancel each other out in the cell counts) in the same image stack.

For comparison, the scatter plot of automated cell counts obtained with the two-dimensional segmentation method (see Section II-D) vs. the manual cell counts is shown in Fig. 5. The scatter plot shows us that the cell count is correct for only 124 (50.8%) image stacks and the MAE is 1.23. It is therefore clear that the results are substantially worse than they are with the K-means segmentation method. In particular, the two-dimensional segmentation method results in a much larger number of false negatives.

IV. DISCUSSION

It is interesting to observe that the K-means step of the proposed K-means segmentation method is akin to methods used for classification of multispectral remotely sensed images and of images obtained by medical imaging techniques such as multispectral magnetic resonance imaging (MRI). In the former case, the images consist of channels that are imaged using radars operating in different bands of electromagnetic waves (radio, infrared, visible), and the pixel values from different bands are used as features in classification; see, for example, [15]. In the latter case, voxel values from images obtained with different parametrization of the scanner are used as features; see, for example, [16].

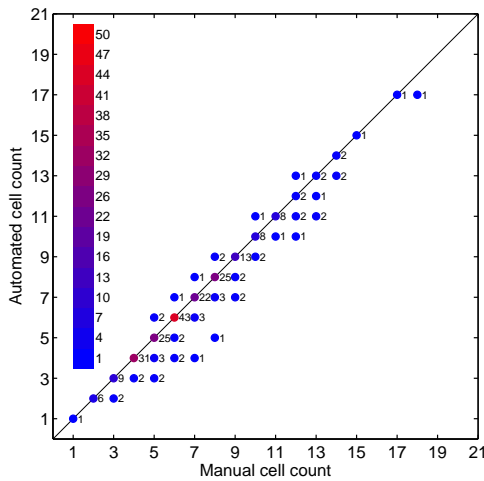


Fig. 4. The scatter plot of automated cell counts obtained with the K-means segmentation method vs. manual cell counts.

The results reported here suggest that additional z -slices help to improve the accuracy of segmentation. Indeed, many of the false negatives in the segmentation results obtained with the two-dimensional method result from the fact that in many cases a single z -slice in which all the cells are in good focus does not exist. On the other hand, some of the segmentation errors of the K-means segmentation method result from the movement of the cells between the times the z -slices were imaged, which is naturally not a problem in the two-dimensional method.

Both segmentation methods have a tendency to result in some false negatives but only few false positives. False positives are damaging irrespective of the application, so their incidence must be minimized in all segmentation schemes. However, in many microscopy applications even a large number of false negatives can be tolerated. For example, if the aim is to obtain statistics on subcellular structures and to associate each of them with a cell, it may not matter that some of the cells are not recognized in segmentation. This means that the statistics on the subcellular structures of these cells cannot be recorded, but since there is usually a practically unlimited supply of cells, this merely means that more images need to be taken so that data on a sufficient number of cells can be obtained.

ACKNOWLEDGMENT

This work was supported by the National Institutes of Health (P50-GM076547) and by the Academy of Finland (application number 213462, Finnish Programme for Centres of Excellence in Research 2006–2011). AN is supported by the Academy of Finland (application number 120325, Researcher Training and Research Abroad). RS is supported by Canadian Institutes for Health Research Fellowship.

REFERENCES

[1] Z. Bar-Joseph, S. Farkash, D. K. Gifford, I. Simon, and R. Rosenfeld, "Deconvolving cell cycle expression data with complementary information," *Bioinformatics*, vol. 20, no. Supplement 1, pp. i23–i30, Aug. 2004.

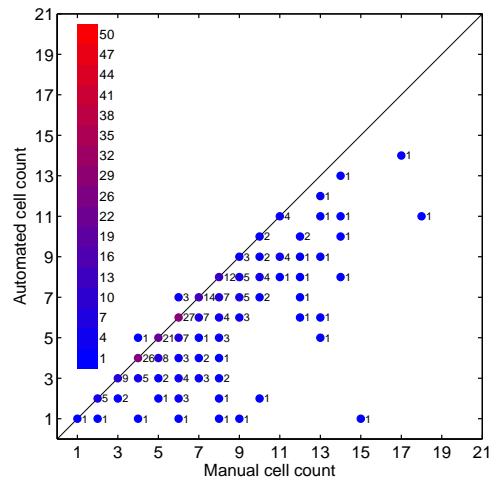


Fig. 5. The scatter plot of automated cell counts obtained by the two-dimensional segmentation method vs. manual cell counts.

[2] S. Cookson, N. Ostroff, W. L. Pang, D. Volfson, and J. Hasty, "Monitoring dynamics of single-cell gene expression over multiple cell cycles," *Mol. Syst. Biol.*, vol. 1, Nov. 2005.

[3] A. Gordon, A. Colman-Lerner, T. E. Chin, K. R. Benjamin, R. C. Yu, and R. Brent, "Single-cell quantification of molecules and rates using open-source microscope-based cytometry," *Nat. Methods*, vol. 4, no. 2, pp. 175–181, Feb. 2007.

[4] M. Kaksonen, C. P. Toret, and D. G. Drubin, "A modular design for the clathrin- and actin-mediated endocytosis machinery," *Cell*, vol. 123, no. 2, pp. 305–230, Oct. 2005.

[5] R. Narayanaswamy, W. Niu, A. D. Scouras, G. T. Hart, J. Davies, A. D. Ellington, V. R. Iyer, and E. M. Marcotte, "Systematic profiling of cellular phenotypes with spotted cell microarrays reveals mating-pheromone response genes," *Genome Biol.*, vol. 7, no. 1, Jan. 2006.

[6] D. G. O'Shea and P. K. Walsh, "The effect of culture conditions on the morphology of the dimorphic yeast *Kluyveromyces marxianus* var. *marxianus* NRRLy2415: a study incorporating image analysis," *Appl. Microbiol. Biotechnol.*, vol. 53, no. 3, pp. 316–322, Mar. 2000.

[7] T. L. Saito, et al., "SCMD: *Saccharomyces cerevisiae* morphological database," *Nucleic Acids Res.*, vol. 32, pp. D319–D322, January 2004.

[8] M. Kaksonen, Y. Sun, and D. G. Drubin, "A pathway for association of receptors, adaptors, and actin during endocytic internalization," *Cell*, vol. 115, no. 4, pp. 475–487, Nov. 2003.

[9] A. Niemistö, T. Aho, H. Thesleff, M. Tiainen, K. Marjanen, M.-L. Linne, and O. Yli-Harja, "Estimation of population effects in synchronized budding yeast experiments," in *Image Processing: Algorithms and Systems II*, ser. Proc. SPIE, vol. 5014, 2003, pp. 448–459.

[10] A. Niemistö, J. Selinummi, R. Saleem, I. Shmulevich, J. Aitchison, and O. Yli-Harja, "Extraction of the number of peroxisomes in yeast cells by automated image analysis," in *Proc. 28th Ann. Int'l Conf. IEEE Engineering in Medicine and Biology Society (EMBC'06)*, New York, USA, Aug. 30 – Sept. 3 2006, pp. 2353–2356.

[11] M. Ohtani, A. Saka, F. Sano, Y. Ohya, and S. Morishita, "Development of image processing program for yeast cell morphology," *J. Bioinform. Comput. Biol.*, vol. 1, no. 4, pp. 695–709, January 2004.

[12] A. Robinson, N. Sadr-kazemi, G. Dickason, and S. T. L. Harrison, "Morphological characterisation of yeast colony growth on solid media using image processing," *Biotechnol. Tech.*, vol. 12, no. 10, pp. 763–767, Oct. 1998.

[13] J. A. Hartigan and M. A. Wong, "A K-means clustering algorithm," *Appl. Stat.*, vol. 28, no. 1, pp. 100–108, 1979.

[14] N. Otsu, "A threshold selection method from gray-level histograms," *IEEE Trans. Syst., Man, Cybern.*, vol. 9, no. 1, pp. 62–66, Jan. 1979.

[15] B. Tso and R. C. Olsen, "Combining spectral and spatial information into hidden Markov models for unsupervised image classification," *Int. J. Remote Sensing*, vol. 26, no. 10, pp. 2113–2133, May 2005.

[16] R. A. D. Carano, A. L. Ross, J. Ross, S. P. Williams, H. Koeppen, R. H. Schwall, and N. van Bruggen, "Quantification of tumor tissue populations by multispectral analysis," *Magn. Reson. Med.*, vol. 51, no. 3, pp. 542–551, Mar. 2004.